Fatigue behavior of hydrogen pre-charged low alloy Cr-Mo steel

Chiara Colombo[a]*, Gabriele Fumagalli[b], Fabio Bolzoni[b], Giorgia Gobbi[a], Laura Vergani[a]

*Corresponding author. E-mail: chiara.colombo@polimi.it. Tel: +390223998667. Fax: +390223998263.

[a] Politecnico di Milano, Department of Mechanical Engineering, Via La Masa 1, 20156 Milan, Italy

[b] Politecnico di Milano, Chemistry, Material and Chemical Engineering Department "Giulio Natta", Via Mancinelli 7, 20131 Milan, Italy

Abstract

Aim of the present work is to study the mechanical behavior in presence of hydrogen of a quenched&tempered low alloy Cr-Mo steel, AISI 4130, used for hydrogen storage and transportation. The sensitivity of steels to hydrogen embrittlement is generally determined by means of two kinds of experimental procedures to hydrogen charge the specimens: gaseous hydrogen in environmental chambers or autoclaves or H_2S solution (recommended by NACE standard). In this work experimental tests are carried out on specimens pre-charged by means of an electrochemical method. A campaign of toughness and fatigue crack growth tests is performed on specimens without and with pre-charged hydrogen. The results are compared and discussed with other, from literature, obtained by following more traditional testing procedures.

By this comparison the adopted experimental procedure, that is safer and easier, seems to provide useful information.

Keywords: Hydrogen embrittlement; hydrogen charging; fatigue crack growth; fracture toughness.

Nomenclature

a	crack length
C, m	coefficients as in Eq.1
E	Young modulus
f	testing frequency
J_{IC}	J toughness without hydrogen
J_H	J toughness with hydrogen
K	stress intensity factor
K_{JIC}	K toughness without hydrogen, evaluated from J_{IC}
K_{JH}	K toughness with hydrogen, evaluated from J_H
K_H	K toughness with hydrogen
N	number of cycles
σ_y	yield strength
σ_{UTS}	ultimate tensile strength

1. Introduction

At present time the increasing energy demand has driven, on the one hand, the development of new oil and gas fields around the world, many of which are sour and, on the other hand, the research of new, sustainable energy sources, as fuel-cell technology, and the use of hydrogen as energy carrier.

These cases involve the utilization of pipelines and huge infrastructures for the transportation of hydrogen or of sour oil and/or hydrocarbon, both dealing with the problem of hydrogen embrittlement.

Up now, this topic is widely debated in literature. Many efforts are made by researchers in order to enhance and deepen the knowledge of this phenomenon through both experimental studies and modelling at different scale. [1-8]

However, the new applications in energy fields require challenging issues for higher operative performances in aggressive working environments, to avoid catastrophic consequences for environment, industrial economy and personnel health. Besides, a full knowledge of the mechanical behavior of metallic materials directly in contact with hydrogen, and in particular a quantification of the hydrogen influence on mechanical properties of steels, is certainly a need for a proper design of these components and structures, as well as to ensure a correct maintenance.

In order to design performing components during their service life up to several years, it is essential to have a reliable database of experimental tests under repeatable testing conditions, referred to the particular environmental conditions where the structure is supposed to work. In literature, such a database is still lacking, due to the complexity of the testing procedure that should simulate the environmental conditions, in which embrittlement happens.

Examples of dangerous environmental conditions are related to the presence of gaseous hydrogen (infrastructure for the storage and transportation of hydrogen) and of acid and sulfide in oil and hydrocarbon, when hydrogen atoms originated from the cathodic reduction reaction can diffuse into the steel (pipelines to export hydrocarbon from sour oil&gas fields).

The experimental procedure should reproduce these conditions to induce the formation of atomic hydrogen on the steel surface. In literature, two different experimental procedures are present: 1) the *in situ* procedure with gaseous hydrogen, 2) the *in situ* procedure with H_2S.

The first procedure uses low (0.1-0.2 MPa, [9, 10, 11]) or high pressure (up to 100 MPa, [12]) gaseous hydrogen in environmental chambers or autoclaves. Firstly, vacuum is created to ensure that the total concentration of background gases, as 0_2, H_20, N_2, would be lower than the concentration of hydrogen. Secondly, the test chamber is filled up with hydrogen, the contaminant gas, and afterwards experimental tests can be performed. Testing equipment is placed inside the chamber: in this way, both static and cyclic loads can be applied to the specimens. Although this procedure ensures a constant hydrogen flow from the specimen surface to its core during the test, and any loading condition (static and cyclic), it requires a source of purified hydrogen and highly controlled testing conditions to be continuously monitored and recorded.

The second procedure is obtained by means of hydrogen sulfide, H_2S in aqueous solutions, and it is recommended in NACE standard TM 0177 [13]. This standard aims giving indications and specification for the optimum selection of materials having minimum susceptibility to *sulfide stress cracking* (SSC) in H_2S environments [14]. Loads are applied during environmental testing: constant load, constant deformation and slow strain rate tests can be performed according to [13]. Particular attention must be paid, since H_2S is highly toxic and not safe, and must be handled with care.

These procedures to hydrogen charge specimens are complex, dangerous and expensive, besides it is difficult to carry out experimental tests as toughness and fatigue crack propagation, unless building *ad hoc* loading frames (*e.g.* [15]).

In this work another experimental procedure has been followed: the electrochemical pre-charge method. By this technique, specimens are hydrogen charged before testing by an electrochemical procedure. Generally, specimens are used as cathodes in a solution, typically acidic, with a defined galvanostatic current density. Newman and Shreir [16] are the authors of one of the first paper dealing with the electrochemical hydrogen charging. A state of the art about hydrogen electrochemical charging is reported in [17].

This pre-charging electrochemical procedure is, of course, safer (no high pressure of gaseous hydrogen or H_2S is required) and less expensive than the other ones. It allows a more convenient experimental set up; in fact, after hydrogen pre-charge the specimens can be tested by using traditional testing equipment.

On the other side, in this type of tests mechanical loading is carried out on hydrogen pre-charged specimens while in NACE stress corrosion crack (SCC) and corrosion fatigue (CF) tests the environmental effect is present at the same time of mechanical loading. In this way, hydrogen is continuously supplied on the metal

surface. It is therefore very important to verify that the effects of the different experimental procedures are comparable and with this aim, a literature survey is performed.

Williams [18] focuses the attention on toughness and fatigue tests, proposing a comparison between the results of experimental tests obtained charging some specimens by low pressure *in situ* gaseous hydrogen system and some other by electrochemical pre-charging method. All specimens are made from AISI 4130 steel. The authors concluded that the two different experimental procedures cause the same embrittlement phenomenon. They found out these conclusions by analyzing both the experimental results (in terms of toughness and fatigue crack growth rate values) and the fracture surfaces. Similar conclusions were confirmed also in a recent work [12], in which fracture surfaces of three different kinds of charging: 1) specimens tested in air; 2) electrochemically hydrogen pre-charged specimens; 3) high-pressure H_2 gas charged specimens are examined.

The material considered in this work is a low alloy Cr-Mo steel, namely AISI 4130. Fatigue crack growth and toughness tests are performed by considering hydrogen pre-charged and hydrogen-free specimens.

Obtained experimental results are compared with other data from literature achieved with the same material and tested in gaseous hydrogen [18, 19]. These authors carried out toughness and fatigue crack growth tests and evidenced the effect of gaseous hydrogen pressure on material mechanical behavior and embrittlement phenomena.

On the contrary, [20] performed experimental tests on AISI 4130 steel, by hydrogen charging the specimens in H_2S aqueous solution.

The results of all these experimental campaigns are compared, with the aim to verify the effectiveness of the pre-charging procedure and even to quantitatively compare the experimental obtained values with equivalent ones from literature.

2. Material

Object of this study is a low alloy Cr-Mo steel (AISI 4130), quenched&tempered, with a tempered martensitic microstructure. Table 1 reports the mechanical properties, obtained from experimental tensile tests, and the chemical compositions.

Table 1. Mechanical properties and chemical composition (%) of AISI 4130 steel.

3. Experimental equipment and setup

The testing procedure is as follows:

- sample machining;
- fatigue pre-cracking. All samples are pre-cracked in air up to approximately a crack length a=2.6 mm;
- hydrogen pre-charging;
- fatigue crack growth or toughness test. All the tests are performed by means of a servo-hydraulic testing machine, MTS Landmark, equipped with a load cell of 100kN capacity. Clip on gage is applied during the tests to measure the crack opening displacements. Measure of crack length is performed by means of the compliance method.

In the present work, specimens are hydrogen pre-charged by an electrochemical technique, adapted from the literature and set up at the Politecnico di Milano. Specimens are cathodically polarized by a constant current density of 0.5 $mA \cdot cm^{-2}$. The solution, deaerated, contains 0.4 $mol \cdot L^{-1}$ of acetic acid (CH_3COOH) and 0.2 $mol \cdot L^{-1}$ of sodium acetate (CH_3COONa), and 600 ppm sulphides, having pH = 4.2; charging time is 20 h. For more details on the charging procedure, see the reference [17]. Figure 1 shows the hydrogen charging equipment.

The hydrogen content in specimens has been measured by using systematically, after each charging, a dummy specimen and the hot glycerol method. This simple and quick method is suitable for a routine control of the diffusible hydrogen content, which resulted always in the range of 1.9-2.7 ppm.

In order to avoid hydrogen degassing, due to diffusion during the interval between the charging operation and the mechanical tests, specimens are stored into liquid nitrogen (T = -196 °C).

The duration of the experimental tests varies based on the type of tests and the imposed test parameters. In particular, the developed tests never exceeded twelve hours. To verify the average hydrogen content still present into the specimens during and after the experimental tests, some measurements of the diffusible hydrogen content with hot glycerol method were carried out on specimens exposed to the air for different times. These results together with the data obtained for dummy specimens measured immediately after the charging procedure are present in Figure 2. This plot represents the hydrogen content as function of H

degassing time. It is possible to note that up to approximately 5 hours after charging, the value of hydrogen content remains quite high (1.3 ppm); this value significantly decreases for longer times (0.3 ppm after 24 hours). Therefore, these data confirm the presence of hydrogen into the specimens also at the end of the tests.

Figure 1. Experimental setup for hydrogen charge.

Figure 2. Diffusible hydrogen content monitored during time. Experimental results evaluated by hot glycerol method.

3.1 Fatigue crack growth tests

Tests are carried out according to ASTM E647-11 standard [21] on single edge-notch C(T) specimens. Figure 3.a shows the dimensions of the specimen. Characteristic dimensions are the width W = 25 mm and the thickness B = 12.5 mm. Fatigue tests are performed in load control, at constant stress ratio R = 0.1 and at room temperature. Three different test frequencies are considered for hydrogen charged specimens: 0.1 Hz, 1 Hz and 10 Hz. In addition, the effect of different initial ΔK on fatigue curves is evaluated in presence of hydrogen.

3.2 Fracture toughness tests

Fracture toughness tests at room temperature are performed following ASTM E1820-09 standard [22]. In this case, the dimensions of C(T) specimens are quite similar to those of fatigue crack growth specimens, unless for the side grooves (Figure 3.b).

Figure 3. Geometry and dimensions in mm of the used C(T) specimens for: **a.** fatigue crack propagation and **b.** toughness tests. Notch angle is 30°; *a* is crack length. 2.5 mm side grooves were machined on specimens for toughness tests.

4. Results and discussion

In this paragraph, results of experimental tests on AISI 4130 specimens are presented and discussed.

4.1 Fatigue crack growth tests

Figure 4 shows experimental results of both uncharged and hydrogen charged specimens in the da/dN–ΔK bi-logarithmic plot.

The uncharged material experiences a trend typical of most common steels, with linearly increasing crack propagation in the entire analyzed ΔK range. To interpolate these data, Paris law is used:

$$\frac{da}{dN} = C \cdot \Delta K^m \tag{1}$$

Parameters C and m are identified through regression. Values are indicated in Table 2, and they are in good agreement with those of [20] obtained on martensitic and bainitic steels. Threshold stress intensity factor ΔK_{th} is found as 7 MPa·m$^{0.5}$.

Figure 4. Results of fatigue crack growth tests on AISI 4130. Hydrogen charged specimens are tested at different testing frequencies.

Table 2. Coefficients of Paris law, calculated for da/dN [m/cycle] and ΔK [MPa$\sqrt{m}$].

Considering hydrogen charged specimens, a different trend can be observed. A general increase in crack growth rate is detected in comparison with the base material (not charged with hydrogen). This is the most visible consequence of the hydrogen presence into the material from the mechanical point of view. Moreover, it is evident that the trend of crack growth rate is characterized by three different stages.

By observing the plot in Figure 4: in correspondence of low ΔK values, crack growth rate rapidly increases (first stage of crack propagation), then, at higher values of ΔK, the slope tends to flatten and to present a plateau region (second stage of crack propagation). Indeed, slopes of da/dN–ΔK in this region reach an order of magnitude lower than the base steel, as indicated in Table 2 parameter m. In the plateau region of the da/dN–ΔK plot, the variation in stress intensity factor ΔK seems having no influence on crack propagation, and the crack experiences a constant growth rate. The plateau region is typical of "stress corrosion fatigue" phenomena, in which there is an interaction between fatigue and stress corrosion cracking [23, 24]. Similar behavior was found by our research group on pipeline carbon and low alloy steels, tested by the same experimental procedure [25, 26, 27].

According to the literature [26, 27], the plateau region of hydrogen charged specimens ends up at very high ΔK values, when the curve for hydrogen charged material tends to the one of the uncharged steel (third stage of crack propagation). This is not fully visible in Figure 4, as specimens failed at lower crack growth rates, but this is a trend well known in the literature. Indeed, in this final part of the test, hydrogen is no more able to accumulate at the crack tip, because of the fast crack growth rate that is controlled only by values of stress intensity factor.

Another parameter influencing crack growth rate in presence of hydrogen is the load frequency. The lower is the frequency, the more pronounced is the embrittlement effect, and the final $da/dN–\Delta K$ curve is shifted upwards, see Figure 4, with respect to the curve of the base material. Especially the curve of H-charged specimens at 0.1 loading frequency shows a strong enhancement of the embrittling effect. This effect is evidenced by values of crack growth rates, which are almost two orders of magnitude higher when compared to the values of the base material (not charged with hydrogen). A trend in $da/dN–\Delta K$ curve is evident from Figure 4: when frequency is increased of one order of magnitude, crack propagation rate is lowered of half order of magnitude. These experimental and macroscopic results can be explained by a consideration at the micro-scale. When the frequency of load application is low, atomic hydrogen has more time to move through the lattice and to reach crack tip, resulting in a macroscopic increase of the embrittling effect.

The obtained results can be compared with literature data from experimental tests carried out on specimens made from the same steel but following different charging and testing procedures.

In the papers [20] and [28] AISI 4130 specimens were fatigue tested in H_2S aqueous solution with similar test parameters. These authors found analogous curves of the crack growth rate. All these results, in fact, are characterized by similar trend: different zones are evident in the diagram as in Figure 4. In presence of hydrogen, crack growth rate is approximately doubled.

This comparison shows that even if the hydrogen charging technique is different from the one used in this work and, in particular, in the literature method the specimens are always in contact with hydrogen during the mechanical tests, the achieved results are comparable.

Figure 5. Influence of different initial ΔK on fatigue crack growth tests on hydrogen-charged AISI 4130; testing frequency: 1 Hz.

All specimens hydrogen charged specimens reported in Figure 4 are tested with the same initial ΔK, approximately equal to 8 MPa·m$^{0.5}$. Separately, Figure 5 evidences the influence of another parameter on fatigue crack growth: the initial ΔK applied during the tests. This plot reports the results of all the hydrogen charged specimens tested at 1 Hz, considering different initial ΔK in a range from 7.1 to 12.3 MPa·m$^{0.5}$. It seems that the higher is the initial ΔK, the higher is also da/dN. Indeed, the curves at the highest initial ΔK are almost overlapped to the ones at low frequency (0.1 Hz) of Figure 4.

4.2 Fracture toughness tests

Experimental tests for fracture toughness measurements are performed according to ASTM E1820-09 standard. Table 3 shows the J and K values obtained by specimens with and without hydrogen.

The J_{IC} value obtained for base material is similar to the literature values. K_H and J_H toughness values from experimental tests carried out on pre-charged specimens are clearly lower than the previous one. The embrittlement effect of hydrogen is evident, causing a reduction in K toughness more than 70%.

Figure 6 shows the trend of experimental load vs vertical load line displacement for two J tests, without and with hydrogen.

Figure 6. J test: load vs displacement curves without and with hydrogen presence.

Table 3. Results of toughness tests.

These fracture toughness values are consistent with those present in literature [18, 19] for specimens of AISI 4130 tested in gaseous hydrogen. In particular Loginow [19] highlighted the effect of pressure of gaseous hydrogen on embrittlement phenomenon on AISI 4130, characterized by yielding stress σ_y=635 MPa, similar to the one tested in this research. We propose to make a comparison between these data and our experimental results by means of the ratio K_H/K_{JIC}, where K_H is the fracture toughness in presence of hydrogen and K_{JIC} is the fracture toughness without hydrogen. From our tests, we determined the ratio K_H/K_{JIC}=0.24. Table 4 highlights values of K_H/K_{JIC} ratio calculated by experimental data in [19] varying hydrogen gaseous pressure. It is possible to note that the result obtained by hydrogen pre-charging method is comparable to those in

gaseous hydrogen at very high pressures, which are the most demanding testing conditions. This confirms that the pre-charging procedure allows achieving the same results of other *in situ* charging method.

Table 4. K_H/K_{JIC} values obtained by experimental data in gaseous hydrogen [19].

4.3 Analysis of the fracture surface

In order to analyze fracture surfaces from toughness and fatigue tests, images are collected by a scanning electron microscopy (SEM). In all these images, the crack propagation is downwards.

Fatigue tests. Fracture surfaces of fatigue specimens tested without hydrogen show brittle aspect, with plane facets; striations can be observed only with high magnifications, see Figure 7. In presence of hydrogen the fracture surfaces show different aspect: in the first stage of the crack propagation, fracture surface is brittle and more fragmented with respect to the specimens without hydrogen; no striations and secondary cracks can be detected, see Figure 8. On the contrary, in the second stage of propagation (high crack propagation rate in the plateau region), fracture becomes partially intergranular with secondary cracks. This is evident in Figure 9, showing images from a specimen charged with hydrogen and tested at 1 Hz. Final fracture is ductile and occurs at high ΔK, after about 15 mm crack growth.

These microscopic observations can clearly support results shown in $da/dN–\Delta K$ plots of Figure 4 and Figure 5. The plateau clearly identifies the region where influence of hydrogen embrittlement is remarkable and crack surface is typically brittle. On the contrary, at the end of the crack propagation, fracture surface and crack growth rate turn back to the original ductile behavior, similar to the base test without hydrogen.

Figure 7. Fracture surface of a hydrogen-free specimen: **a.** pre-crack and **b.** details with striations.

Figure 8. Fracture surface for a specimen charged with hydrogen **a.** at 0.5 mm from the pre-crack, 1 Hz, and **b.** magnification.

Figure 9. Fracture surface for a specimen charged with hydrogen **a.** in the initial stage and **b.** at 3 mm from pre-cracking.

In literature, several authors examined the fracture surfaces of hydrogen charged specimens, by SEM observations. All the available micrographs are similar to the previous ones, independently on the charging procedure.

Tau [16] finds similar fracture surfaces by examining 4130 hydrogen charged specimens. The specimens are hydrogen charged and tested in H_2S aqueous solution. The fracture is predominantly intergranular and irregular.

Williams [18] examines the fracture surfaces of 4130 specimens fatigue tested in gaseous hydrogen. The aspect of these fracture surfaces is close to the one detected in the present work. At low stress intensity factors (corresponding to the first stage of crack propagation), the fracture is intergranular with some minor deformation evidence on the intergranular facets. At stress intensity factors corresponding to the second stage the fracture is primarily intergranular with some evidence of ductile failure. Close to the transition zone (between the second and third stage) the fracture surface contains large zones exhibiting multiple dimples with a few areas somewhat intergranular.

In [29] representative fractographs of 4130 tested in gaseous hydrogen show an aspect close to ones of the present work. The fracture surfaces contain a large amount of integranular separation along the prior austenitic grains, deformation markings and secondary cracks.

J integral tests. Different specimens have been observed, showing some common behavior:

- at the fatigue pre-crack tip there is no evidence of ductile tearing or blunting of the crack;
- the first propagation stage is brittle, with different modes: integranular (prior austenitic grains), or with little fragmented facets (Figure 10); secondary cracks are visible in both modes;
- in both lateral surfaces brittle fracture is similar to the previous one and it is initiated from “side grooves” , as we can see in Figure 11;
- the fracture proceeds in a ductile way with low toughness; dimples are fine and mainly nucleated by non-metallic inclusions or second phases (Figure 12.a). Sometimes “cellular” fracture is observed (Figure 12.b), similar to the morphology found in the paper [26] for carbon and low alloy pipeline steels.

Figure 10. Fracture surface after *J*–Δ*a* tests for a specimen charged with hydrogen: brittle surface.

Figure 11. Fracture surface after *J*–Δ*a* tests for a specimen charged with hydrogen: brittle crack initiation from side groove.

Figure 12. Fracture surface after *J*–Δ*a* tests for a specimen charged with hydrogen: ductile surface (final fracture).

5. Conclusions

An electrochemical procedure was followed to hydrogen pre-charge specimens made from low alloy Cr-Mo steel AISI 4130. A campaign of experimental tests was performed, with the aim to define the sensitivity of the steel to hydrogen embrittlement and to compare the pre-charge procedure followed in these tests with the other commonly used, based on gaseous hydrogen and H_2S environment.

The following conclusions can be drawn:

- Low alloy Cr-Mo AISI 4130 steel shows a high sensitivity to hydrogen embrittlement: in specimens charged with hydrogen, fatigue crack growth rate is two or three order of magnitude higher. The trend of crack growth rate as a function of ΔK is composed by three main zones: a rapid initial increase in growth rate, followed by a plateau, with constant values of crack growth rate, and a last zone where the crack growth rate is rapidly increasing. The effect of frequency is evident, too: at lower loading frequencies (0.1 to 1 Hz) crack growth rates are higher with respect to the higher test frequencies (10 Hz).
- The toughness K_H was decreased to 1/4 in value in presence of hydrogen.
- Fracture surface of fatigue specimens charged with hydrogen is brittle and more fragmented with respect to the specimens without hydrogen; no striations and secondary cracks can be detected; in the second stage of propagation fracture becomes partially intergranular with secondary cracks.
- The comparison of the results obtained by different test procedures (pre-charging, exposure to H_2S containing environment and presence of gaseous hydrogen) shows a good agreement of the results. The electrochemical pre-charging method seems to be enough conservative with respect to gaseous hydrogen exposure.

Acknowledgement

Our group thanks Francesca Brunella for her help and support in the collection of fracture surfaces images and in their analysis.

References

[1] Troiano A. The role of hydrogen and other interstitials in the mechanical behavior of metals. Trans ASM 1960; 52:54-80.

[2] Beachem C. A new model for hydrogen-assisted cracking (hydrogen embrittlement). Metallurgical and Materials Transactions B 1972; 3:441-455.

[3] Lynch S. Mechanisms of hydrogen-assisted cracking. Proceedings of Metals Forum 1979; 2:189-200.

[4] Gangloff RP, Somerday BP. Gaseous Hydrogen Embrittlement of Materials in Energy Technologies. Woodhead publishing, Cambridge UK, 2012.

[5] Murakami Y, Kanezaki T, Mine Y, Matsuoka S. Hydrogen embrittlement mechanism in fatigue of austenitic stainless steels. Metallurgical and Materials Transaction A, 2008; 39:1327-1339.

[6] Kanezaki T, Narazaki C, Mine Y, Matsuoka S, Murakami Y. Effects of hydrogen on fatigue crack growth behavior of austenitic stainless steels. International Journal of Hydrogen Energy, 2008; 33:2604-2619.

[7] Murakami Y, Matsuoka S. Effect of hydrogen on fatigue crack growth of metals. Engineering Fracture Mechanics, 2010; 77:1926–1940.

[8] Vergani L, Colombo C, Gobbi G, Bolzoni FM, Fumagalli G. Hydrogen effect on fatigue behavior of a quenched&tempered steel. Procedia Engineering 2014; 74:468-471.

[9] Frandsen JD, Marcus HL. Environmentally Assisted Fatigue Crack Propagation in Steel. Metall Mater Trans Phys Metall Mater Sci 1977; 8A:265-272.

[10] Gangloff RP, Wei RP. Gaseous Hydrogen Embrittlement of High Strength Steels. Metallurgical transactions A 1977;8A: 1043-1053.

[11] Oda Y, Noguchi H. Observation of hydrogen effects on fatigue crack growth behavior in an 18Cr-8Ni austenitic stainless steel. International Journal of Fracture 2005; 132:99–113.

[12] Neeraj T, Srinivasan T, Li J. Hydrogen embrittlement of ferritic steels: Observations on deformation microstructure, nanoscale dimples and failure by nanovoiding. Acta Materialia 2012; 60:5160-5171.

[13] NACE Standard TM0177-96: Laboratory Testing of Metals for Resistance to Sulfide Stress Cracking and Stress Corrosion Cracking in H_2S Environments.

[14] EFC Publication nr. 16. Guidelines on materials requirements for carbon and low alloy steels for H_2S-containing environments in oil and gas production. 2009.

[15] Sun Z, Moriconi C, Benoit G, Halm D, Hénaff G. Fatigue crack growth under high pressure of gaseous hydrogen in a 15-5PH martensitic stainless steel: influence of pressure and loading frequency. Metall Mater Trans Phys Metall Mater Sci 2013: 44A: 1320-1330.

[16] Newman JF, Shreir LL. Role of hydrides in hydrogen entry into steel from solutions containing promoters. Corrosion Science 1977; 9: 631-641.

[17] Bolzoni F, Fassina P, Fumagalli G, Lazzari L, Re G. Hydrogen charging of carbon and low alloy steel by electrochemical methods. Proceedings of European Corrosion Congress EUROCORR 2010, September 13–17, Moscow.

[18] Williams DP, Nelson HG. Embrittlement of 4130 steel by low-pressure gaseous hydrogen. Metallurgical Transactions 1970. 1:63-78.

[19] Loginow AW, Phelps EE. Steels for seamless hydrogen pressure vessels. Corrosion 1975; 31:404-412.

[20] Tau L, Chan SLI, Shin CS. Hydrogen enhanced fatigue crack propagation of bainitic and tempered martensitic steels. Corrosion Science 1996. 38:2049-2060.

[21] ASTM E647-11: Standard test method for measurement of fatigue crack growth rates.

[22] ASTM E1820-09: Standard test method for measurement of fracture toughness.

[23] McEvily AJ, Wei RP. Fracture mechanics and corrosion fatigue. In: Devereux O, McEvily AJ, Staehle RW. Corrosion Fatigue: chemistry, mechanics and microstructure. Houston: National Association of Corrosion Engineers; 1972, p. 381-395.

[24] Sinigaglia D, Re G, Pedeferri P. Cedimento per fatica e ambientale dei materiali metallici. Milano: CLUP; 1979.

[25] Fassina P, Bolzoni F, Fumagalli G, Lazzari L, Vergani L, Sciuccati A. Influence of hydrogen and low temperature on mechanical behaviour of two pipeline steels. Engineering Fracture Mechanics 2012; 81:43-55.

[26] Fassina P, Brunella MF, Lazzari L, Re G, Vergani L, Sciuccati A. Effect of Hydrogen and low temperature on fatigue crack growth of pipeline steels. Engineering Fracture Mechanics 2013; 103:10-25.

[27] Vergani L, Sciuccati A, Re G, Bolzoni F. Effect of Hydrogen Environment on Fatigue Behaviour of High Toughness Steels. In: Tang P, Zhang JL. Fatigue Crack Growth: Mechanisms, Behavior and Analysis. NOVA Publishers. 2012.

[28] Zhang YL, Miao W, Sun ZY, Wang J, Zeng YJ. Fatigue crack growth behavior of 4130X steel in H_2S environment. Corrosion Engineering, Science and Technology 2009; 44:462-468.

[29] Simmons GW, Pao PS, and Wei RP. Fracture mechanics and surface chemistry studies of subcritical crack growth in AISI 4340 steel. Metallurgical Transactions A, 1978; 9:1147-1158.

Figures

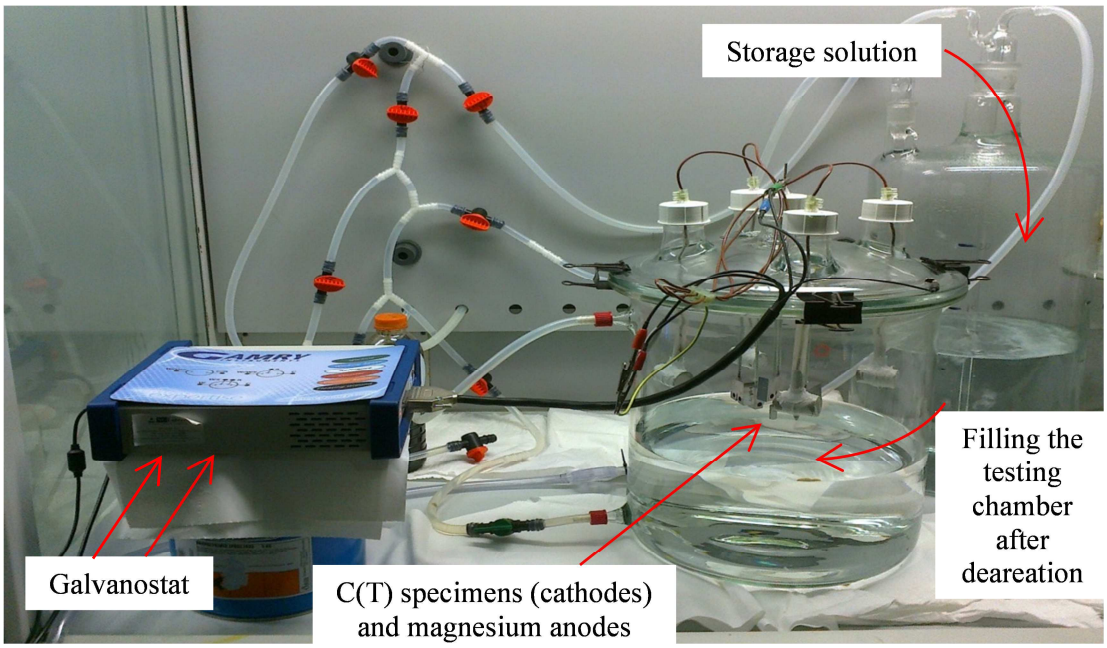

Figure 1. Experimental setup for hydrogen charge.

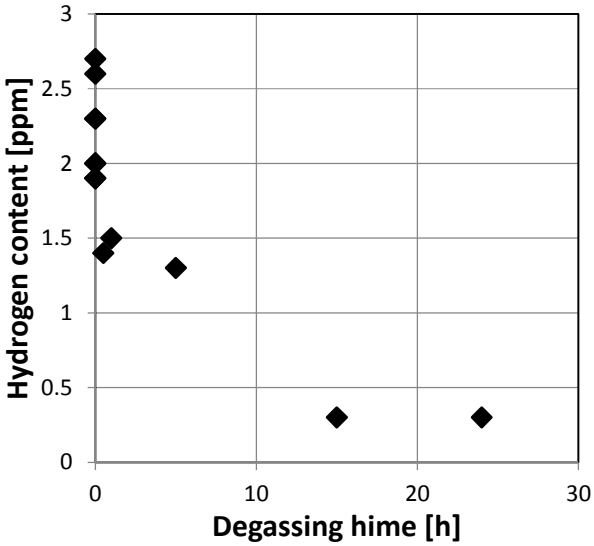

Figure 2. Diffusible hydrogen content monitored versus time. Experimental results evaluated by hot glycerol method.

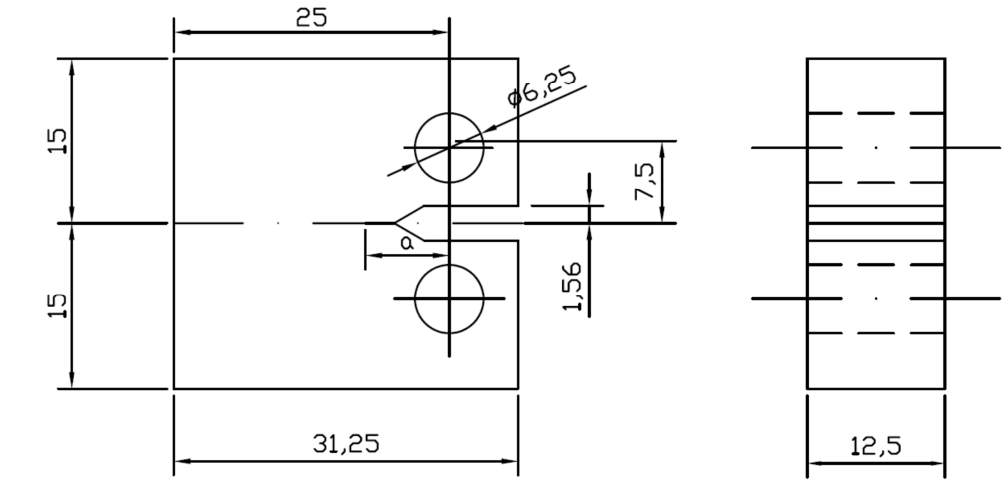

a.

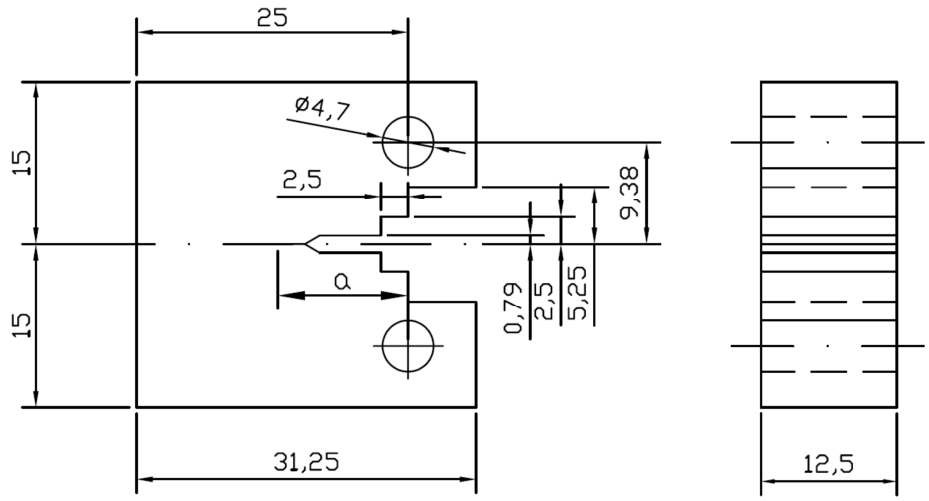

b.

Figure 3. Geometry and dimensions in mm of the used C(T) specimens for: **a.** fatigue crack propagation and **b.** toughness tests. Notch angle is 30°; *a* is crack length. 2.5 mm side grooves were machined on specimens for toughness tests.

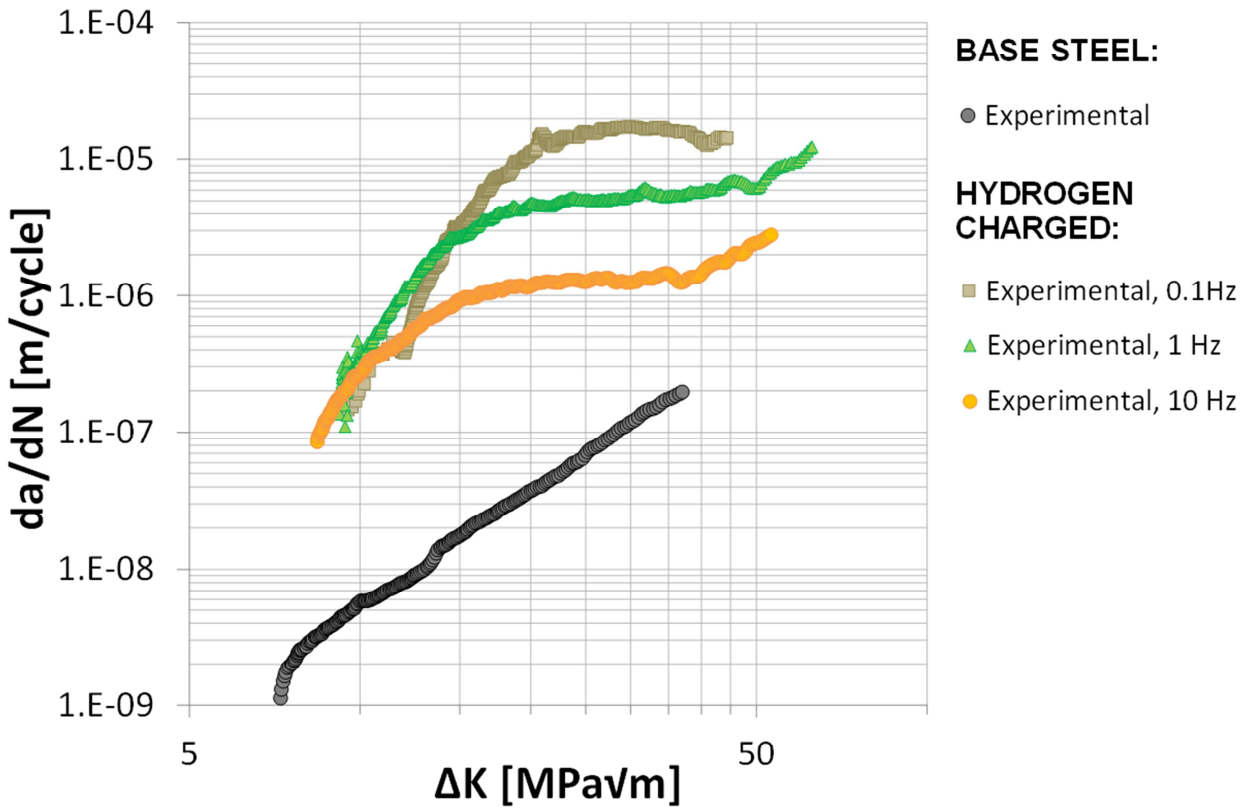

Figure 4. Results of fatigue crack growth tests on AISI 4130. Hydrogen charged specimens are tested at different testing frequencies.

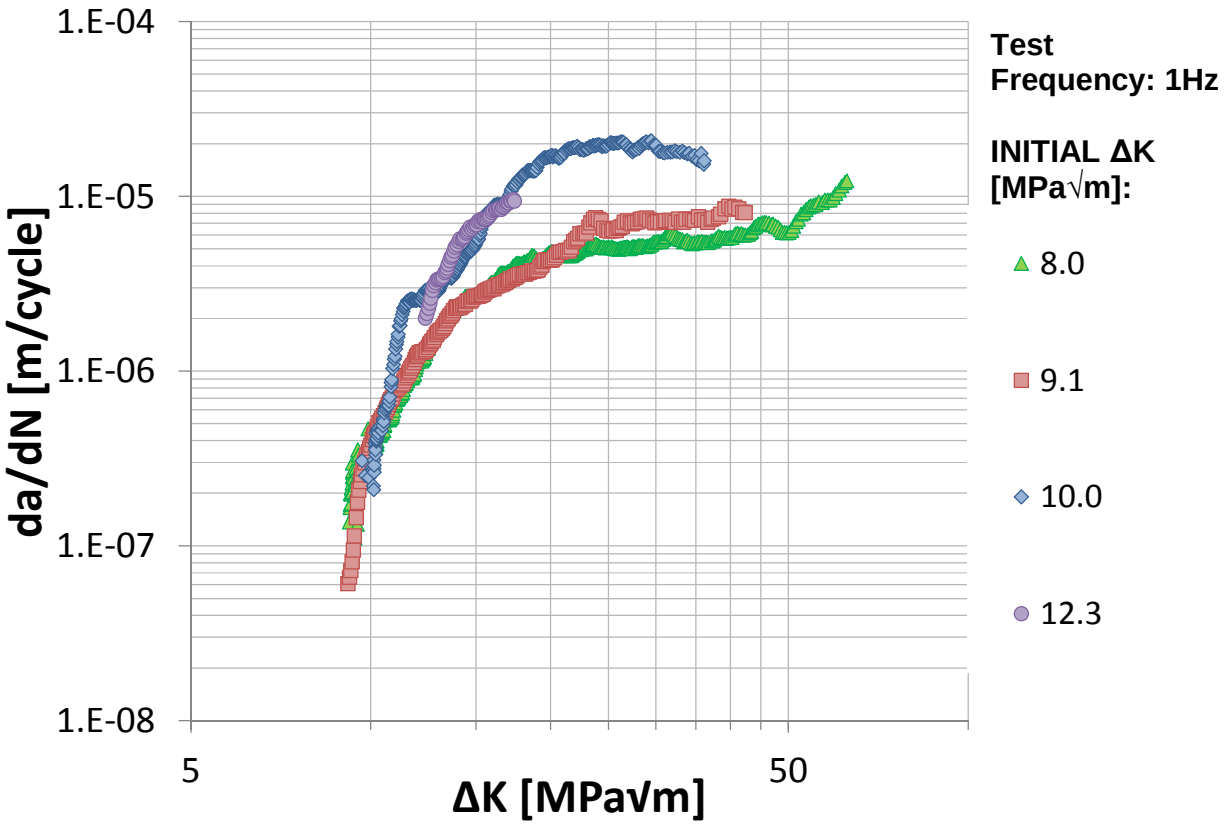

Figure 5. Influence of different initial ΔK on fatigue crack growth tests on hydrogen-charged AISI 4130; testing frequency: 1 Hz.

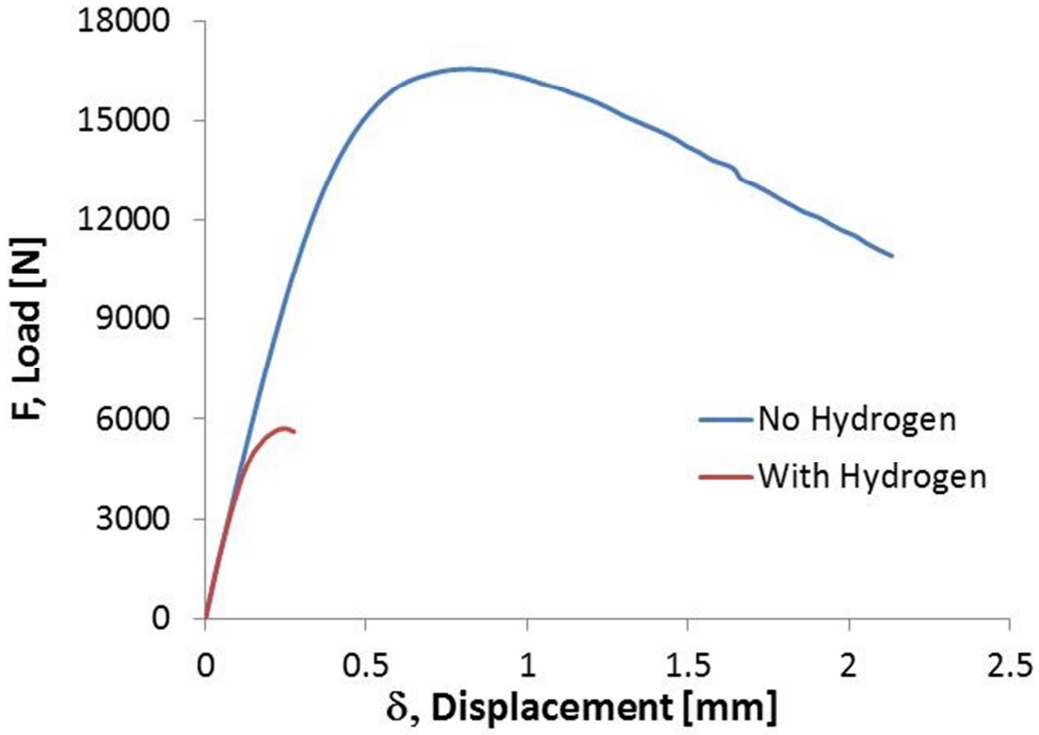

Figure 6. *J* test: load vs displacement curves without and with hydrogen presence.

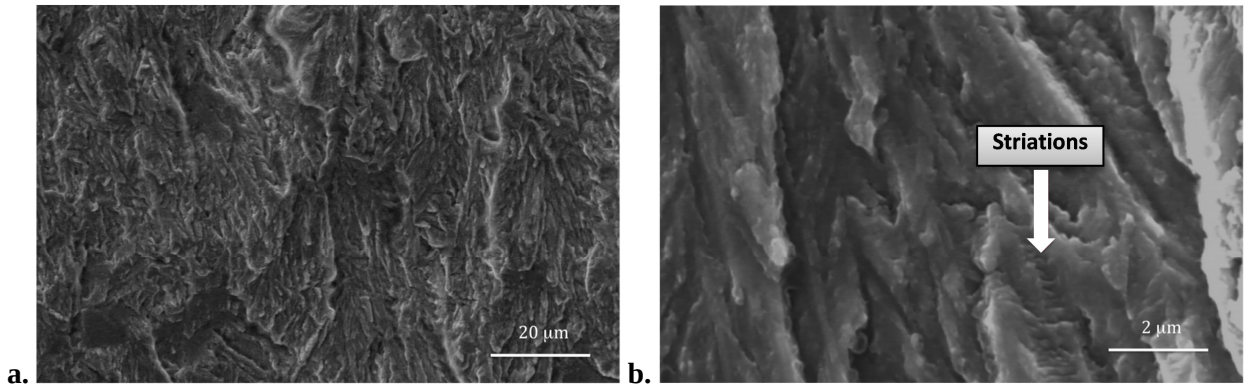

Figure 7. Fracture surface of a hydrogen-free specimen: **a.** pre-crack and **b.** details with striations.

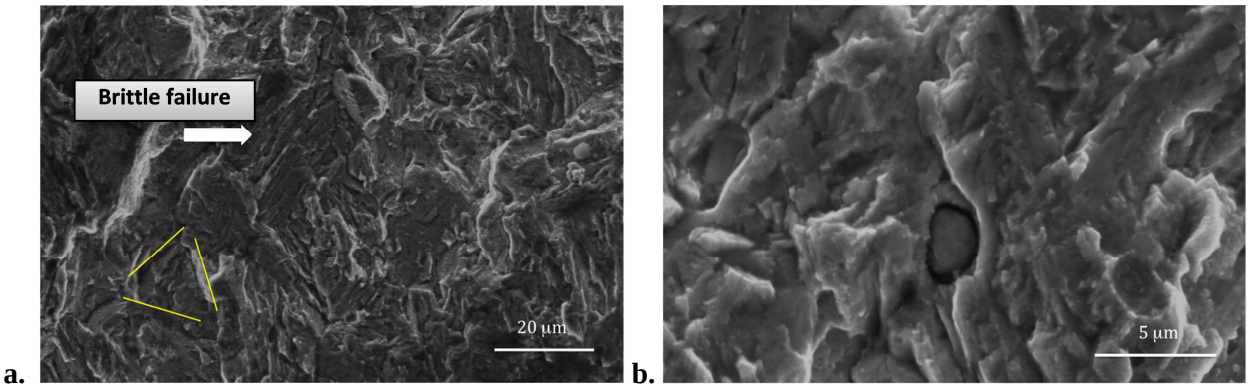

Figure 8. Fracture surface for a specimen charged with hydrogen **a.** at 0.5 mm from the pre-crack, 1 Hz, and **b.** magnification.

a. 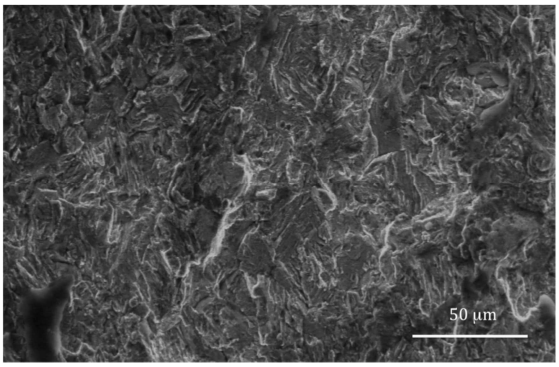

b. 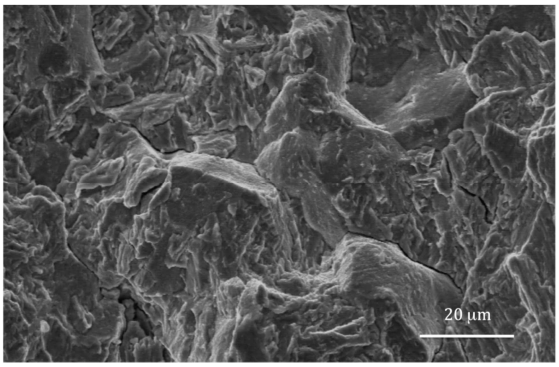

Figure 9. Fracture surface for a specimen charged with hydrogen **a.** in the initial stage and **b.** at 3 mm from pre-cracking.

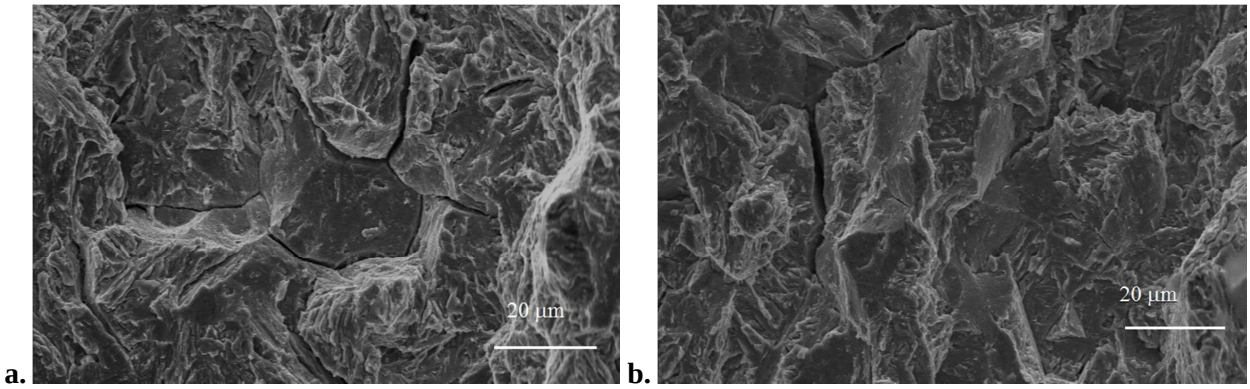

Figure 10. Fracture surface after *J*–Δ*a* tests for a specimen charged with hydrogen: brittle surface.

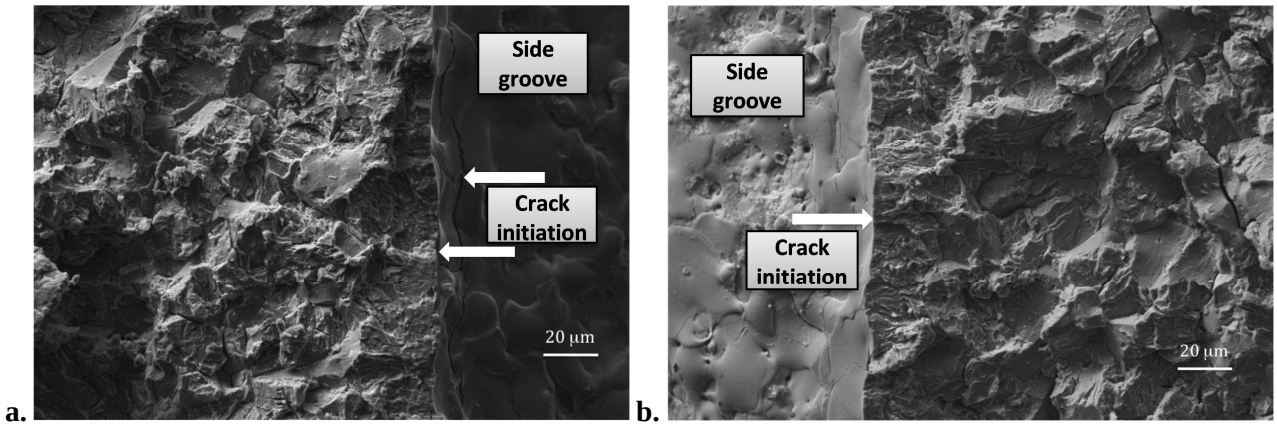

Figure 11. Fracture surface after *J*–Δ*a* tests for a specimen charged with hydrogen: brittle crack initiation from side groove.

a. 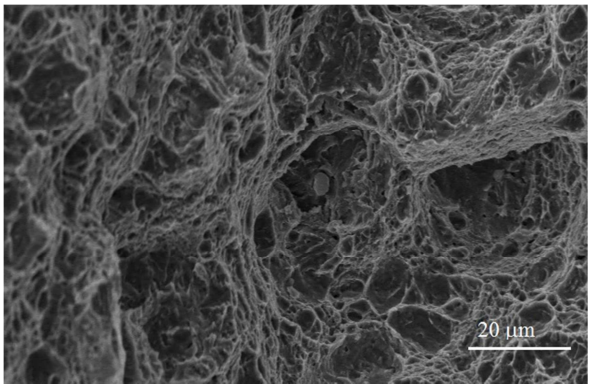

b. 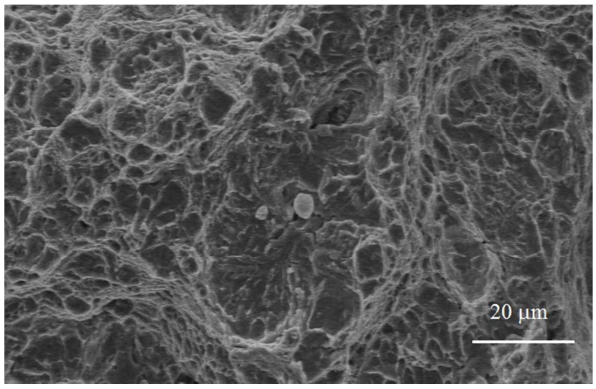

Figure 12. Fracture surface after *J*–Δ*a* tests for a specimen charged with hydrogen: ductile surface (final fracture).

Tables

Table 1. Mechanical properties and chemical composition (%) of AISI 4130 steel.

σ_y [MPa]	σ_{UTS} [MPa]	E [MPa]
715	950	220000

C	Mn	Si	Cr	Mo
0.30	0.50	0.25	0.95	0.20

Table 2. Coefficients of Paris law, calculated for da/dN [m/cycle] and ΔK [MPa$\sqrt{m}$].

* This scatter depends on the initial ΔK, as shown in Figure 5.

	***f* [Hz]**	***C***	***m***
Base		7e-12	2.868
H-charged	0.1	5e-6	0.365 (plateau)
	1	2e-6 ÷ 1e-5 *	0.155 ÷ 0.357 (plateau) *
	10	7e-7	0.200 (plateau)

Table 3. Results of toughness tests.

Base	J_{IC} **[N/mm]** 215.5	K_{JIC} **[MPa$\sqrt{m}$]** 217.7
H-charged	- J_H **[N/mm]** 22.0	K_H **[MPa$\sqrt{m}$]** 38.8 46.6 K_{JH} **[MPa$\sqrt{m}$]** 69.9

Table 4. K_H/K_{JIC} values obtained by experimental data in gaseous hydrogen [19].

H_2 gas pressure [MPa]	K_H/K_{JIC}
0	1
21	0.704
41	0.544
62	0.360
69	0.256
97	0.416